International Journal of Pharmaceutics, 15 (1983) 37–48
Elsevier Biomedical Press

Determination of the rearrangement kinetics of chloramphenicol-3-monosuccinate using an automated HPLC system

William A. Wargin and Dale Eric Wurster

School of Pharmacy, University of North Carolina, Chapel Hill, NC 27514 (U.S.A.)

(Received June 11th, 1982)
(Accepted November 1st, 1982)

Summary

The kinetics of the rearrangement of chloramphenicol-3-monosuccinate to chloramphenicol-1-monosuccinate were studied as a function of pH (5.0–8.0), temperature (25, 37, 50°C), and ionic strength (0.1–0.5 M). A microcomputer-controlled injector was used to sample the reaction medium at predetermined time intervals and to immediately load the sample onto a reversed-phase HPLC column. The rearrangement was catalyzed by hydroxide ion and ionic strength effects were observed. Although activation energies varied slightly with pOH, the activation energies for the forward and reverse reactions were within 3.6% of each other at any given pOH. Calculation of the enthalpies and entropies of activation for the forward and reverse reactions yielded slight differences in enthalpies (< 3.7%) and appreciable differences in entropies (1.9–3.5 e.u.). The observed differences in k_f and k_r were therefore attributed to steric hindrance in the formation of the 1-ester.

Introduction

Chloramphenicol-3-monosuccinate ($CAPS_3$) is a prodrug used for intravenous administration. Hydrolysis of $CAPS_3$ in the liver produces the active moiety, chloramphenicol (CAP). Sandmann et al. (1968, 1970) reported that $CAPS_3$ exists in equilibrium with another molecular form, a cyclic hemi-ortho ester, at neutral pH. It has recently been shown (Brent et al., 1980) that $CAPS_3$ rearranges to chloramphenicol-1-monosuccinate ($CAPS_1$) (Fig. 1), with the cyclic hemi-ortho ester being a likely intermediate. This rearrangement occurs under conditions existing in solutions intended for intravenous administration and under physiological condi-

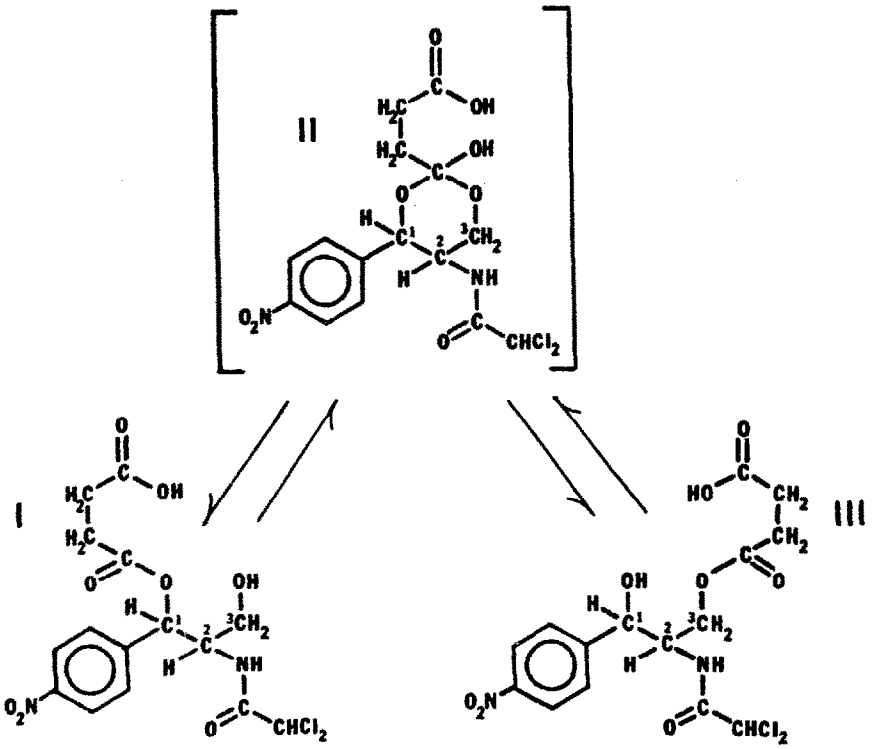

Fig. 1. Structures of: chloramphenicol-3-monosuccinate (III), cyclic hemi-ortho este: (II), and chloramphenicol-1-monosuccinate (I).

tions in vivo (Burke et al., 1980). The factors affecting this rearrangement have not been studied in detail.

Materials and methods

An automated HPLC procedure was used to study the kinetics of the rearrangement of $CAPS_3$ to $CAPS_1$ (Fig. 2). Reaction medium was continuously pumped[1] through a 15 μl fixed-volume loop injector[2]. Actuation of the injector at the desired times was accomplished with a 48k microcomputer[3] and custom interface. Circulation of reaction medium occurred at a rate of 1.50 ml/min, the total volume of the circulation loop being 0.84 ml, and the time required for a sample to reach the injector loop after entering the circulation loop was 0.31 min.

Mobile phase (acetonitrile–phosphate buffer 28 : 72) adjusted to a pH of 5.55 with concentrated phosphoric acid was delivered by a second pump[1] through the injector and subsequently to a reversed-phase HPLC column[4]. The mobile phase

[1] Milton Roy Mini-Pump, Laboratory Data Control, Riviera Beach, FL 33404.
[2] Micromeritics Model 735 with Model 725 automatic injector valve, Micromeritics, Norcross, GA 30093.
[3] Model I, Level II, 48K Radio Shack Computer, Tandy, Forth Worth, TX 76102.
[4] RP-18, 10-μm particle size, Alltech Associates, Deerfield, IL 60015.

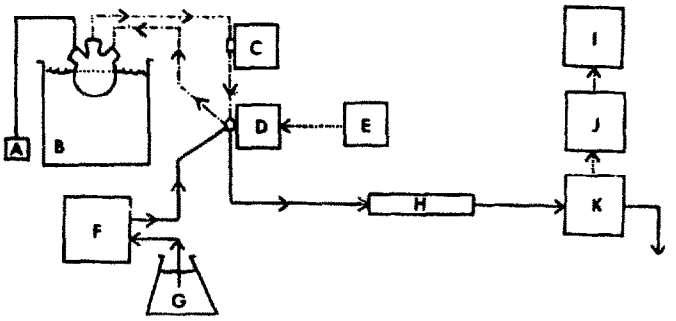

Fig. 2. Schematic of analytical system: digital thermometer[9] (A), reaction vessel in thermostatted waterbath (B), pump for transfer of reaction medium (C), injector (D), microcomputer and interface (E), HPLC pump (F), mobile phase reservoir (G), reversed-phase HPLC column (H), stripchart recorder (I), integrator (J), UV absorption detector (K), sample flow (·–·–·), mobile phase flow (———), and electrical signal (· · · · · ·).

[9] Fischerbrand Digital Thermometer, Fischer Scientific, Pittsburgh, PA 15238.

flow rate was 1.20 ml/min. Column eluent was monitored by a UV detector[5] at 280 nm. The areas under the chromatographic peaks were automatically integrated[6] and the peaks were displayed on a strip-chart recorder[7]. The mobile phase pH of 5.55 resulted in baseline resolution of $CAPS_1$, $CAPS_3$ and CAP. At this pH no significant rearrangement occurred during the chromatographic process. The retention times were 5.2 min for $CAPS_1$, 7.4 min for $CAPS_3$, and 9.6 min for CAP.

The influence of pH and temperature on the rearrangement was studied at an ionic strength of 0.500 M. Reaction media with pH values of 5.00, 6.00, 7.00, 7.40 and 8.00 ± 0.02 consisted of phosphate buffer (0.0667 M) and appropriate quantities of sodium chloride. Temperatures of 25.0, 37.0 and 50.0 ± 0.1°C were maintained with a heater-mixer[8]. The influence of ionic strength was studied at 37.0°C at each pH value. Ionic strengths ranging from 0.100 to 0.500 M were utilized. The possibility of buffer catalysis was investigated at each pH value; temperature and ionic strength were maintained constant at 37.0°C and 0.500 M, respectively. Buffer concentrations were 0.0667 and 0.1334 M.

Adjustment of the ionic strength of the reaction media required that a determination of the dissociation constant for the second dissociation of phosphoric acid be made at experimental conditions. This was accomplished according to the method of Finholt et al. (1965). At an ionic strength of 0.500 M the pK_a for the second dissociation was found to be a 6.65 at 25.0°C, 6.60 at 37.0°C, and 6.58 at 50.0°C. These are in excellent agreement with the value of 6.54 determined by Finholt et al. (1965) at an ionic strength of 0.5 M and a temperature of 60°C.

To each 200 ml of reaction media 20 mg (4.73×10^{-5} mol) of $CAPS_3$ were added. The concentration of $CAPS_3$ was too small to have a measurable effect on the ionic

[5] Model 5480 UV Monitor, Glenco Scientific, Houston, TX 77007.

[6] CDS-111, Varian Instruments, Sunnyvale, CA 94086.

[7] Fisher Recordall, Houston Instruments, Austin, TX.

[8] Thermomix 1420, B. Braun, Melsungen, F.R.G.

strength. A determination of the pK_a (method of Finholt et al., 1965) of $CAPS_3$ at 25.0, 37.0, and 50.0°C and ionic strength equal to 0.500 M was made, however, so that the percentage of ionized drug would be known at each experimental pH. At each temperature value the experimentally determined pK_a was 4.30. Any change in pK_a over the relatively narrow temperature range encompassed was apparently smaller than the analytical error for the method employed. Using the Henderson-Hasselbalch relationship, it was determined that $CAPS_3$ was at least 83.4% ionized at all experimental pH values.

Kinetic analysis

The molar absorptivities of $CAPS_1$ and $CAPS_3$ were shown to be equal by summing the integrated areas for the peaks representing $CAPS_1$ and $CAPS_3$ at each sample time. Constancy of the sums of the areas indicated equal molar absorptivities. This was advantageous since mole fractions of $CAPS_1$ could be obtained directly from:

$$R = \frac{I}{I + III} \tag{1}$$

where R = mole fraction of $CAPS_1$, I = integrated area of $CAPS_1$ peak, and III = integrated area of $CAPS_3$ peak.

A typical rearrangement chromatogram is shown in Fig. 3. The formation of $CAPS_1$ appeared to follow first-order kinetics. Plots of log(amount remaining to be reacted) vs time were used to verify the apparent first-order kinetics. Plots were linear with r^2 values greater than 0.9964.

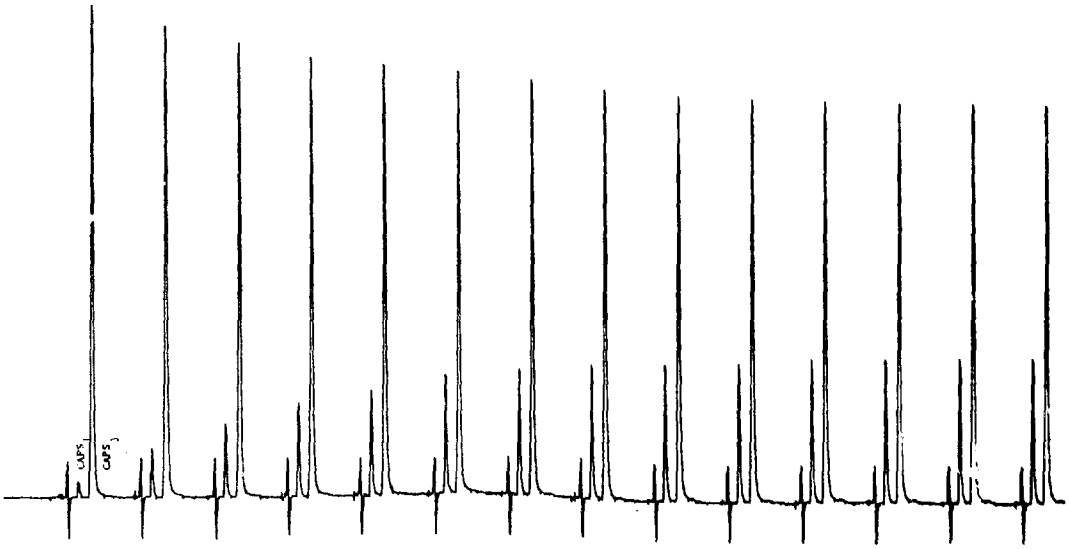

Fig. 3. A typical rearrangement chromatogram. The first peak after the injection front is $CAPS_1$, the second peak is $CAPS_3$.

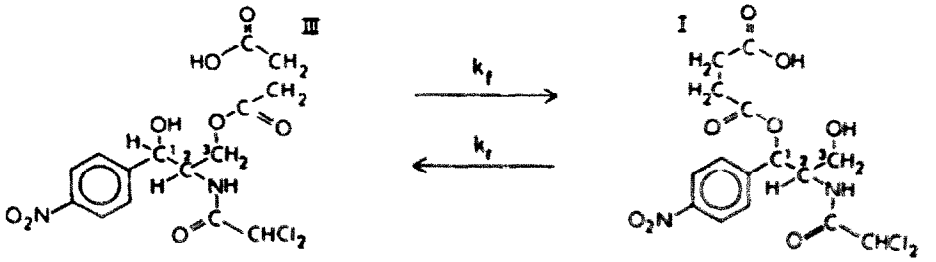

Fig. 4. Rearrangement model used to generate Eqns. 2 and 3.

Development of a proper model required knowing whether or not the rearrangement was reversible. Reversibility was demonstrated by isolating $CAPS_1$ by HPLC and then running the rearrangement reaction with this isolated $CAPS_1$. At equilibrium, the mole fraction of $CAPS_1$ obtained was equal to the mole fraction of $CAPS_1$ obtained when $CAPS_3$ was the starting material. Loss of $CAPS_3$ or $CAPS_1$ to

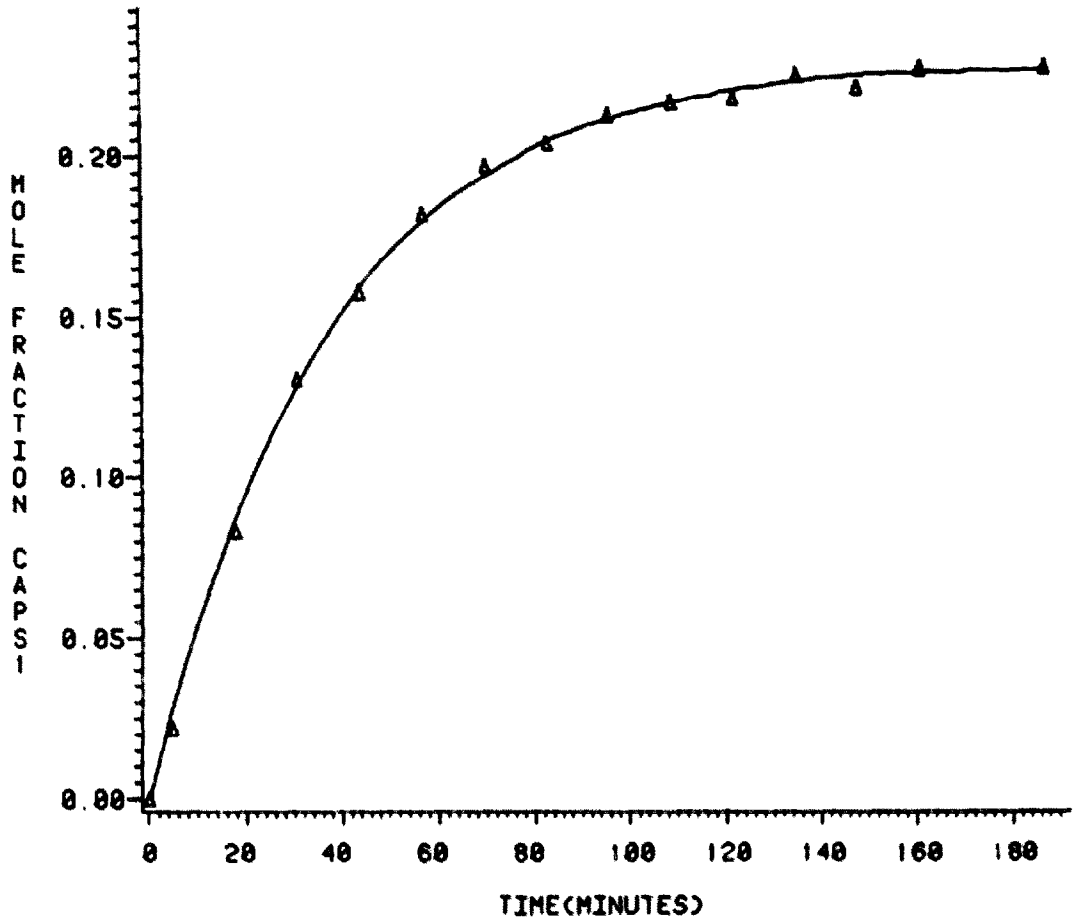

Fig. 5. Typical non-linear least-squares regression analysis curve fit. Symbols are data points, curve is the fitted curve. Plot represents a single pH = 7.00, temperature = 37.0°C, ionic strength = 0.500 M run.

CAP could be neglected since formation of CAP was very slow compared to the rearrangement reaction at all reaction conditions. The resultant model is shown in Figure 4.

Eqns. 2 and 3 describe, respectively, the concentrations of $CAPS_3$ and $CAPS_1$ with time where $[CAPS_3]_0$ is the concentration of $CAPS_3$ at zero time.

$$[CAPS_3] = \frac{[CAPS_3]_0 k_r}{k_f + k_r} + \frac{[CAPS_3]_0 k_f}{k_f + k_r} \cdot e^{-(k_f + k_r)t} \tag{2}$$

$$[CAPS_1] = \frac{[CAPS_3]_0 k_f}{k_f + k_r} - \frac{[CAPS_3]_0 k_f}{k_f + k_r} \cdot e^{-(k_f + k_r)t} \tag{3}$$

Simultaneous solution of Eqns. 2 and 3 for the mole fraction of $CAPS_1$ (R) yielded:

$$R = \frac{k_f}{k_f + k_r}(1 - e^{-(k_f + k_r)t}) = B0(1 - e^{-B1t}) \tag{4}$$

where $B0 = k_f/(k_f + k_r)$, and $B1 = k_f + k_r$. Estimates of B0 and B1 were obtained by non-linear least-squares regression analysis[10] of mole fraction–time data. Such analysis resulted in curve fits (see example, Fig. 5) with r^2 values ranging from 0.9979 to 0.9999. Values of k_f and k_r were calculated from the estimates of B0 and B1.

The use of mole fraction data obtained directly from peak areas in such an analysis provides two distinct advantages. First, no internal standard is required. Second, formation of a small amount of CAP during the rearrangement reaction does not affect the calculated values of k_f and k_r.

Results and Discussion

The automated system for chemical kinetic analysis used in this study provided several advantages over manual sampling. The system permitted unattended sampling at desired time intervals. Equally spaced sample intervals were obtained over long time periods (days) thus allowing a more accurate characterization of the reaction profile. Continuous pumping of reaction medium through the fixed-volume injector loop provided excellent reproducibility, immediate sample analysis (i.e. no additional rearrangement after sampling), and minimal sample size. Importantly, several manual analyses indicated that the sampling system used had no untoward effects (such as catalysis) on the calculated rate constants.

The apparent reaction rate constants for the forward and reverse reactions are shown in Table 1 for all experimental combinations of pH, temperature, ionic strength, and total buffer concentration. All rate constants represent the average of

[10] Proc NLIN, Statistical Analysis System, Raleigh, NC 27605.

TABLE I

AVERAGED APPARENT REACTION RATE CONSTANTS

pH	Temperature (°C)	Ionic strength (M)	Total buffer concentration (M)	k_f (min^{-1})	k_r (min^{-1})
5.00	25.0	0.500	0.0667	5.36×10^{-5}	1.82×10^{-4}
5.00	37.0	0.500	0.0667	1.99×10^{-4}	6.88×10^{-4}
5.00	50.0	0.500	0.0667	7.09×10^{-4}	2.44×10^{-3}
5.00	37.0	0.300	0.0667	1.92×10^{-4}	6.66×10^{-4}
5.00	37.0	0.100	0.0667	1.87×10^{-4}	6.50×10^{-4}
5.00	37.0	0.500	0.1334	2.16×10^{-4}	7.53×10^{-4}
6.00	25.0	0.500	0.0667	2.39×10^{-4}	7.94×10^{-4}
6.00	37.0	0.500	0.0667	8.93×10^{-4}	3.01×10^{-3}
6.00	50.0	0.500	0.0667	3.07×10^{-3}	1.05×10^{-2}
6.00	37.0	0.300	0.0667	7.80×10^{-4}	2.63×10^{-3}
6.00	37.0	0.100	0.0667	4.70×10^{-4}	1.58×10^{-3}
6.00	37.0	0.500	0.1334	9.40×10^{-4}	3.32×10^{-3}
7.00	25.0	0.500	0.0667	1.79×10^{-3}	5.98×10^{-3}
7.00	37.0	0.500	0.0667	6.50×10^{-3}	2.18×10^{-2}
7.00	50.0	0.500	0.0667	2.23×10^{-2}	7.56×10^{-2}
7.00	37.0	0.261	0.0667	5.33×10^{-3}	1.78×10^{-2}
7.00	37.0	0.161	0.0667	3.46×10^{-3}	1.15×10^{-2}
7.00	37.0	0.500	0.1334	6.52×10^{-3}	2.20×10^{-2}
7.40	25.0	0.500	0.0667	4.42×10^{-3}	1.47×10^{-2}
7.40	37.0	0.500	0.0667	1.58×10^{-2}	5.30×10^{-2}
7.40	50.0	0.500	0.0667	5.22×10^{-2}	1.79×10^{-1}
7.40	37.0	0.282	0.0667	1.31×10^{-2}	4.44×10^{-2}
7.40	37.0	0.182	0.0667	8.96×10^{-3}	2.98×10^{-2}
7.40	37.0	0.500	0.1334	1.52×10^{-2}	4.94×10^{-2}
8.00	25.0	0.500	0.0667	1.60×10^{-2}	5.36×10^{-2}
8.00	37.0	0.500	0.0667	5.58×10^{-2}	1.86×10^{-1}
8.00	50.0	0.500	0.0667	1.67×10^{-1}	5.60×10^{-1}
8.00	37.0	0.295	0.0667	6.52×10^{-2}	1.90×10^{-1}
8.00	37.0	0.195	0.0667	3.94×10^{-2}	1.30×10^{-1}
8.00	37.0	0.500	0.1334	5.48×10^{-2}	1.84×10^{-1}

multiple determinations with each individual determination of k_f and k_r having been obtained according to the procedure outlined in the 'Kinetic analysis' section.

The mole fraction of $CAPS_t$ at equilibrium was found to be 0.230 ± 0.007. This equilibrium position was independent of all experimental variables.

Plots of log $k_{overall}$ vs pH were constructed for the 25.0, 37.0, and 50.0°C, $\mu = 0.500$ M data (Fig. 6). $k_{overall}$ represents the rate of approach to equilibrium and is the sum of k_f and k_r. The dependence of log $k_{overall}$ on pH is linear ($r^2 \geq 0.9994$) between pH = 6.00 and pH = 8.00 at all 3 temperatures with the average slope being 0.89. This behavior indicates the presence of specific base catalysis. The dependence

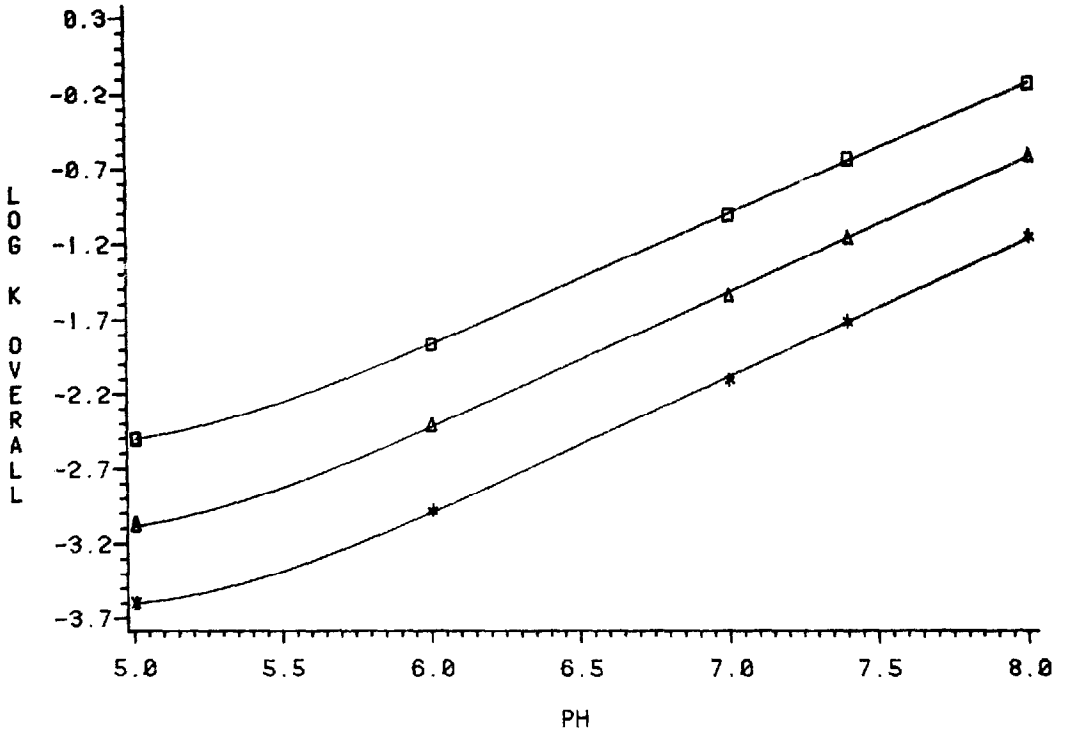

Fig. 6. pH profile for the rearrangement of $CAPS_3$ to $CAPS_1$ at ionic strength = 0.500 M and temperature = 50.0°C (□), 37.0°C (△), and 25.0°C (*).

of log $k_{overall}$ on pH becomes non-linear at pH = 5.00. This non-linearity can most likely be attributed to the solvent-catalyzed reaction becoming significant. The rearrangement of $CAPS_3$ to $CAPS_1$ does not exhibit the V-shaped profile that is characteristic of ester hydrolysis. A run conducted at pH = 2.00, temperature = 50.0°C and $\mu = 0.500$ M failed to yield any $CAPS_1$ after 7 h. If rearrangement occurs at all in this pH range, it is exceedingly slow and there is no evidence for specific acid catalysis. Neither of the phosphate buffer species was found to be catalytic at any of the experimental pH values.

The effect of ionic strength on the rate of reaction was evaluated at 37.0°C at each pH value. Plots (Fig. 7) of log $k_{overall}$ vs square-root of μ showed that effects were present at pH values of 6.00, 7.00, 7.40 and 8.00. This is consistent with specific base catalysis of an ionized species. The effect of ionic strength was not linear over the range of ionic strengths employed. This non-linearity was expected since the theory of Bronsted and Bjerrum actually applies to the range of square-root of $\mu < 0.2$. Rates of reaction were essentially independent of ionic strength at pH = 5.00. $CAPS_3$ is still 83.4% ionized, but the solvent-catalyzed reaction now contributes appreciably to the apparent forward and reverse reaction rate constants.

In order to determine the true second-order reaction rate constants for the forward and reverse reactions it was necessary to know the actual hydroxide ion

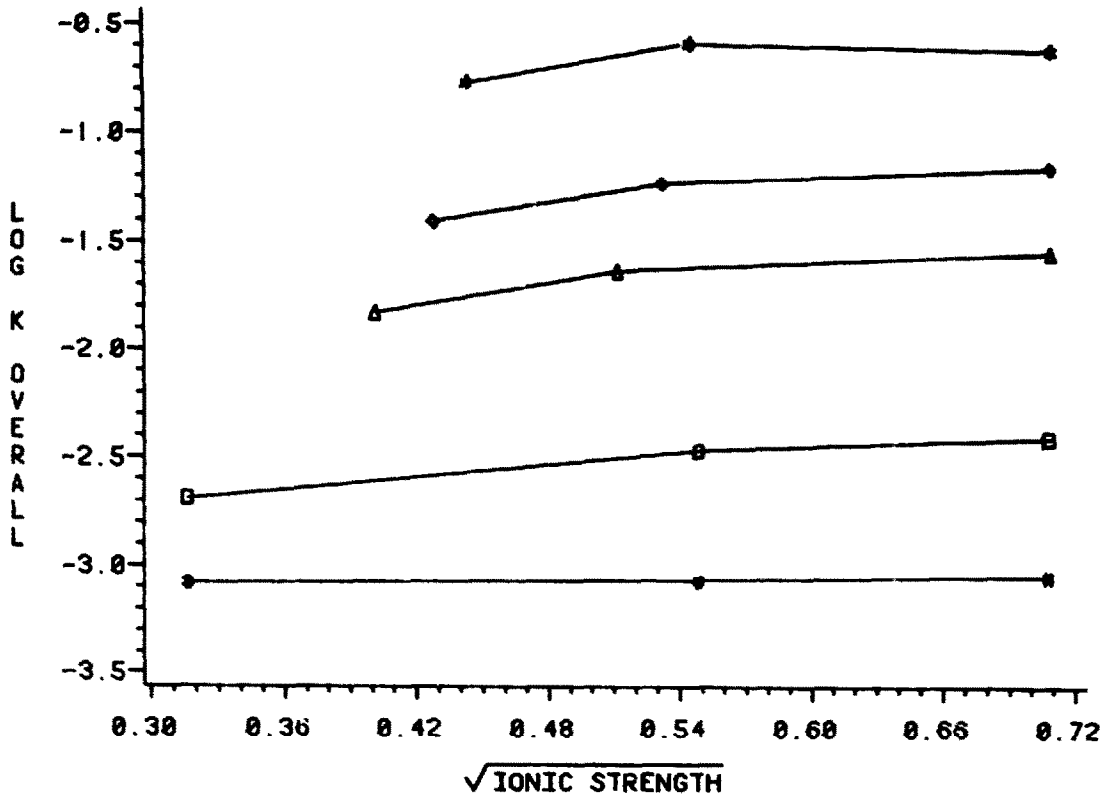

Fig. 7. Effect of ionic strength on reaction rate constant. Temperature = 37.0°C and pH = 8.00 (*), 7.40 (◇), 7.00 (△), 6.00 (□), and 5.00 (#).

concentration at each combination of pH and temperature (ionic strength constant at 0.500 M). Hydroxide ion concentrations were calculated using the ionic activity coefficients and ionization constants determined by Harned and Hamer (1933). It was also desired to have the apparent rate constants (k_f and k_r) represent the same hydroxyl ion concentrations regardless of temperature. Therefore, the logarithms of the experimentally determined values of k_f and k_r were linearly regressed against the calculated pOH values over the linear range of the pOH profile (i.e. a total of 6 plots were made, log k_f vs pOH at 25.0°C, log k_r vs pOH at 25.0°C, log k_f vs pOH at 37.0°C, log k_r vs pOH at 37.0°C, log k_f vs pOH at 50.0°C, log k_r vs pOH at 50.0°C). The rate constants at the desired pOH values were taken from the fitted lines.

The apparent rate constants (k_f and k_r) for the pH = 5.00 data had to be treated somewhat differently since they were not linear functions of pOH. Additionally, it was necessary to separate both k_f and k_r into rate constants representing the specific base-catalyzed reaction and rate constants representing the solvent-catalyzed reaction. The values of k_f and k_r at the desired pOH were obtained graphically. The forward and reverse apparent rate constants for specific base catalysis at the desired pOH were obtained by extrapolation of the linear plots of log k vs pOH described in

the previous paragraph. The rate constants for solvent catalysis at the desired pOH were then obtained from the relation:

$$k_{apparent} = k_{solvent} + k_{apparent,base} \tag{5}$$

True second-order rate constants were calculated for all rate constants representing specific base catalysis:

$$k_{true} = k_{apparent}/[-OH] \tag{6}$$

These rate constants are shown in Table 2.

Activation energies for the foward and reverse reactions at each value of pOH were determined according to the Arrhenius relationship:

$$\log k = \log A - \frac{E_a}{2.303RT} \tag{7}$$

Plots of the data representing the forward, specific base-catalyzed reactions, the

TABLE 2

AVERAGED SECOND-ORDER REACTION RATE CONSTANTS (μ = 0.500 M)

pOH	Temperature (K)	$k_{f,2nd}$ ($l \cdot mol^{-1} \cdot min^{-1}$)	$k_{r,2nd}$ ($l \cdot mol^{-1} \cdot min^{-1}$)
5.18	298.16	0.98×10^{4}	3.30×10^{4}
5.18	310.16	1.53×10^{4}	5.10×10^{4}
5.18	323.16	2.56×10^{4}	8.61×10^{4}
5.78	298.16	1.11×10^{4}	3.71×10^{4}
5.78	310.16	1.76×10^{4}	5.88×10^{4}
5.78	323.16	3.06×10^{4}	10.35×10^{4}
6.18	298.16	1.20×10^{4}	4.02×10^{4}
6.18	310.16	1.93×10^{4}	6.49×10^{4}
6.18	323.16	3.44×10^{4}	11.71×10^{4}
7.18	298.16	1.47×10^{4}	4.89×10^{4}
7.18	310.16	2.44×10^{4}	8.24×10^{4}
7.18	323.16	4.64×10^{4}	15.94×10^{4}
8.18	298.16	1.79×10^{4}	5.95×10^{4}
8.18	310.16	3.08×10^{4}	10.48×10^{4}
8.18	323.16	6.25×10^{4}	21.68×10^{4}
8.18 *	298.16	2.77×10^{-5}	0.96×10^{-4}
8.18 *	310.16	9.84×10^{-5}	3.42×10^{-4}
8.18 *	323.16	29.58×10^{-5}	10.08×10^{-4}

* These values are for the forward and reverse solvent-catalyzed reactions. Therefore, the rate constants are first-order rate constants (min^{-1}).

reverse, specific base-catalyzed reactions, and the forward and reverse solvent-catalyzed reactions were made. Linear least-squares regression analysis was used to determine the slopes of the lines which best fit the data ($r^2 \geq 0.9910$). It can be seen from Table 3 that the activation energy for the specific base-catalyzed reaction varies with pOH and that the largest value of E_a is associated with the solvent-catalyzed reaction. More importantly, the activation energies for each forward–reverse reaction pair are very close to being equal, the maximum difference being 3.6%. The slight differences observed, if significant, favor the forward reaction. It is apparent that activation energy considerations cannot explain the relatively small mole fraction of $CAPS_1$ at equilibrium. A reasonable speculation would be that steric hindrance at the 1-position is responsible for the differences in the forward and reverse reaction rate constants. If so, this effect should be manifested by differences in the entropies of activation for the forward and reverse reactions.

The rate constant for a reaction can be expressed in terms of the enthalpy of activation and the entropy of activation according to the equation:

$$k = \frac{RT}{N_0 h}\left(e^{\Delta S^*/R}\right)\left(e^{-\Delta H^*/RT}\right) \tag{8}$$

where N_0 = Avogadro's number, h = Planck's constant, ΔS^* = entropy of activation, and ΔH^* = enthalpy of activation. Division of both sides of the equation by T followed by log transformation yields:

$$\log\left(\frac{k}{T}\right) = \log\left(\frac{R}{N_0 h}\right) + \frac{\Delta S^*}{2.303R} - \frac{\Delta H^*}{2.303RT} \tag{9}$$

This equation is similar in form to the working form of the Arrhenius equation and a plot of log(k/T) versus 1/T allows the enthalpy of activation to be calculated from the slope of the line. The y-intercept of the same line is used to calculate the entropy of activation.

Plots of the data representing the forward, specific base-catalyzed reactions, the

TABLE 3

ENERGIES, ENTHALPIES AND ENTROPIES OF ACTIVATION

pOH	$E_{a,f}$ (cal/mol)	$E_{a,r}$ (cal/mol)	ΔH_f^* (cal/mol)	ΔH_r^* (cal/mol)	ΔS_f^* (e.u.)	ΔS_r^* (e.u.)
5.18	7320	7340	6700	6730	−26.0	−23.5
5.78	7770	7860	7150	7240	−24.2	−21.5
6.18	8070	8200	7450	7580	−23.0	−20.2
7.18	8810	9050	8200	8430	−20.2	−17.0
8.18	9560	9900	8950	9280	−17.3	−13.8
8.18 *	18,140	17,960	17,520	17,350	−28.7	−26.8

* Solvent-catalyzed reaction.

reverse, specific base-catalyzed reactions, and the forward and reverse solvent-catalyzed reactions were made. Linear least-squares regression analysis was used to determine the slopes and intercepts of the lines which best fit the data ($r^2 \geq 0.9950$).

The results in Table 3 show that, as would be predicted from the activation energy results, there is essentially no difference in the enthalpy of activation for a forward–reverse reaction pair ($\leq 3.7\%$).

The entropies of activation are different between the forward and reverse reactions at a given pOH. Depending on the type of reaction and the pOH, this difference ranges from 1.9 e.u. to 3.5 e.u. In all cases $\Delta S_f^{\neq}$ is more negative than $\Delta S_r^{\neq}$. These results are consistent with the hypothesis that steric hindrance is responsible for the forward reaction being much slower than the reverse reaction and, therefore, the relatively small mole fraction of $CAPS_1$ at equilibrium.

Acknowledgements

The authors wish to express their appreciation to Mr. Nels W. Marvin for the design and construction of the custom interface and associated software. The authors also wish to thank Dr. Edward J. Randinitis of Warner-Lambert Company for the gift of the chloramphenicol-3-monosuccinate.

References

Brent, D.A., Chandrasurin, P., Ragouzeous, A., Hurlbert, B.S. and Burke, J.T., Rearrangement of chloramphenicol-3-monosuccinate. J. Pharm. Sci., 69 (1980) 906–908.

Burke, J.T., Wargin, W.A. and Blum, M.R., High-pressure liquid chromatographic assay for chloramphenicol, chloramphenicol-3-monosuccinate, and chloramphenicol-1-monosuccinate. J. Pharm. Sci., 69 (1980) 909–912.

Finholt, P., Jurgensen, G. and Kristiansen, H., Catalytic effect of buffers on degradation of penicillin G in aqueous solution. J. Pharm. Sci., 54 (1965) 387–393.

Harned, H.S. and Hamer, W.J., The ionization constant of water and the dissociation of water in potassium chloride solutions from electromotive forces of cells without liquid junction. J. Am. Chem. Soc., 55 (1933) 2194–2206.

Sandmann, B.J., The chemistry of chloramphenicol-3-monosuccinate, Doctoral Dissertation, University of Winsconsin, 1968.

Sandmann, B., Szulczewski, D., Windheuser, J. and Higuchi, T., Rearrangement of chloramphenicol-3-monosuccinate. J. Pharm. Sci., 59 (1970) 427–429.